WILEY-VCH

Approaching the Glass Transition Temperature of GeTe by Crystallizing $Ge_{15}Te_{85}$

*Julian Pries, Yuan Yu, Peter Kerres, Maria Häser, Simon Steinberg, Fabian Gladisch, Shuai Wei, Pierre Lucas, Matthias Wuttig**

J. Pries, Dr. Y. Yu, P. Kerres, M. Häser, Prof. M. Wuttig
Institute of Physics IA, RWTH Aachen University, 52074 Aachen, Germany
E-mail: wuttig@physik.rwth-aachen.de
Dr. S. Steinberg, F. Gladisch
Institute of Chemistry, RWTH Aachen University, 52074 Aachen, Germany
Prof. S. Wei
Department of Chemistry, Aarhus University, DK-8000 Aarhus-C, Denmark
Prof. P. Lucas
Department of Materials Science and Engineering, University of Arizona, Tucson, AZ, 85721, United States

Keywords: Undercooled liquid, glass transition, phase change materials, crystallization kinetics

Like many Phase Change Materials, GeTe crystallizes upon heating at a conventional rate before the calorimetric glass transition is reached. This has so far prevented an unambiguous determination of its glass transition temperature T_g. Here, a new approach is realized to estimate the glass transition temperature T_g for GeTe through progressive crystallization of $Ge_{15}Te_{85}$. Selective crystallization of pure tellurium during sub-T_g annealing leads to a gradual change in the composition of the amorphous surrounding towards that of GeTe. This gives rise to a new endotherm whose onset temperature gradually approaches the T_g of GeTe.

1. Introduction

Phase Change Materials (PCMs) such as GeTe or Sb_2Te_3 are a class of materials that can be switched rapidly between two solid phases [1, 2]. These two solid phases, namely the amorphous and crystalline phase, feature a contrast in optical and electrical properties that makes them suitable for optical and electrical data storage devices [2]. This property contrast was previously explained by a change in chemical bonding: While the amorphous phase is

covalently bonded [3], the crystalline phase shows metavalent bonding (MVB) [4-6]. To improve data transfer rates, a comprehensive understanding of crystallization kinetics is crucial [7]. Specifying the viscosity's temperature dependence is of major interest for this purpose since the nucleation rate I and crystal growth velocity v_g are inversely proportional to viscosity η [8-12]. To describe the viscosity as a function of temperature of the liquid and undercooled liquid phase (UCL) [13] the fragility m [14] and the glass transition temperature T_g of the material are essential. The fragility can be given by [14, 15]

$$m = \left. \frac{\mathrm{d} \log_{10} \eta}{d\, T_g/T} \right|_{T=T_g} . \quad (1)$$

Unfortunately, values of T_g for GeTe reported in literature vary from as low as 150 °C up to 230 °C [16-21]. This large variation results in a large and unfavorable uncertainty when it comes to predicting crystallization kinetics for PCM-based data storage devices. For this reason, an accurate value based on experimental data for the glass transition temperature T_g of GeTe is highly desirable.

2. Results

An attempt at measuring the glass transition temperature of amorphous GeTe is shown in **Figure 1**. Here, amorphous powder prepared by magnetron sputter deposition was heated in a Differential Scanning Calorimeter (DSC) at a constant heating rate of 40 K/min after annealing at increasing temperatures for 1 h. As Figure 1 shows, the DSC trace of the un-annealed (as-deposited) GeTe exhibits a broad exotherm starting at around 95 °C, before crystallization is initiated at 165 °C. Upon annealing up to 115 °C, the crystallization remains largely unaffected, while the exotherm prior to crystallization progressively disappears. This is a well-established consequence of enthalpy release from the glassy phase due to structural relaxation in hyperquenched glasses and it has been observed in other PCMs like $Ge_2Sb_2Te_5$ [22, 23], chalcogenide [22, 24], oxide [25, 26], metallic glasses [27] and other glasses before.

However, instead of showing a glass transition endotherm following the relaxation exotherm, crystallization sets in. Thus obscuring any thermal event that could have signaled a glass transition. Therefore, it becomes clear that the glass transition temperature of amorphous GeTe cannot be directly measured from heating due to fast crystallization.

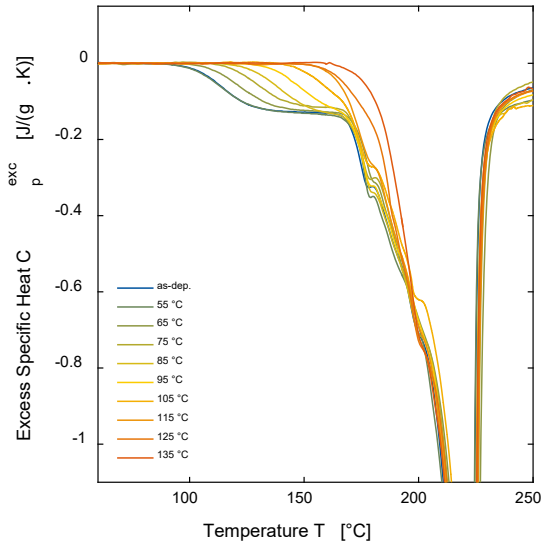

Figure 1: Excess heat capacity C_p^{exc} of amorphous GeTe powder obtained by DSC after an annealing at the indicated temperature for one hour followed by heating with a rate ϑ_h of 40 K/min. Upon heating amorphous GeTe starts releasing heat due to structural relaxation beginning at 95 °C for the as-deposited state. Crystallization is initiated at about 165 °C for all heat treatments depicted and shows its maximum at 223 °C. There are two shoulders in the crystallization exotherm: one at 180 °C and the other at around 200 °C. While the exothermic heat release prior to crystallization indicates structural relaxation of the glassy amorphous state, the glass transition is not observed before crystallization starts.

A similar enthalpy relaxation phenomenon is observed in **Figure 2** a) and b) for $Ge_{15}Te_{85}$. As for GeTe, the enthalpy release caused by structural relaxation of the glassy phase is largely influenced by annealing. This is expected as long as the annealing temperature is below the glass transition temperature of the material (or to be precise, its fictive temperature T_f) [28]. Differing from that in GeTe, in $Ge_{15}Te_{85}$ the exothermic heat release is followed by a glass transition without crystallization interfering. The glass transition temperature T_g can be measured from the onset of the glass transition to be 135 °C for the un-annealed (as-deposited) material, see Figure 2, which is close to the T_g of the melt-quenched glass of the same composition [24, 29]. Following the glass transition, the material enters and remains in

the UCL up to the onset of crystallization at around 185 °C. Interestingly, there are two exothermic crystallization events peaking at 220 and 230 °C.

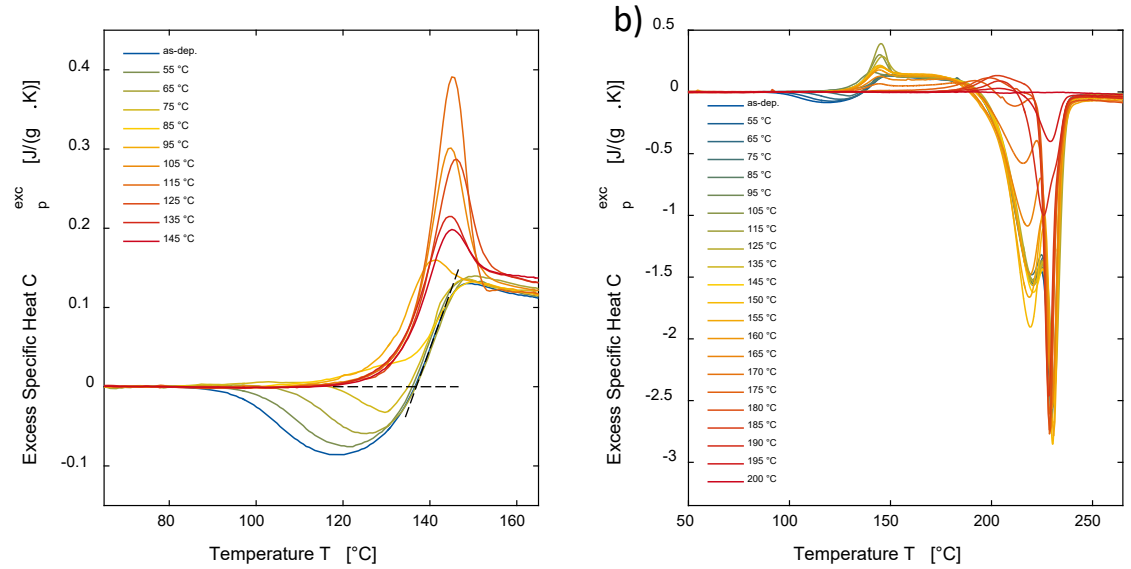

Figure 2: Excess heat capacity C_p^{exc} of amorphous $Ge_{15}Te_{85}$ powder obtained by DSC after an annealing at the indicated temperature for one hour and subsequent heating with a rate of ϑ_h of 40 K/min. Similar to Figure 1, in a) the exothermic heat release due to structural relaxation of the glassy phase is visible starting at 90 °C for the as-deposited phase. The enthalpy relaxation exotherm is followed by the glass transition with a glass transition temperature T_g of 135 °C (as-dep.). The onset construction to obtain the glass transition temperature is depicted by the dashed lines. The undercooled liquid (UCL) is observed in between the glass transition and the onset of crystallization at about 185 °C, see b). Note that crystallization consists of two individual processes indicated by the two distinct peaks with peak temperatures of 220 °C and 230 °C. Besides the changes to the glass transition induced by annealing, the first crystallization peak can be removed completely by annealing at 185 °C for 1 h, while the second peak remains unaffected. At this annealing temperature, an unexpected endotherm is observed around 200 °C, see b).

As the annealing temperature increases, the enthalpy trapped during quenching is progressively released and the relaxation exotherm develops into an endothermic overshoot. When the annealing temperature becomes larger than T_g, the material enters the UCL during annealing and since the UCL is a (meta-)stable equilibrium phase, annealing does not lead to any further enthalpy decrease [28]. When cooled again at a constant cooling rate of 40 K/min, the UCL vitrifies and the resulting glasses feature the same enthalpy state. Therefore, the excess heat capacity C_p^{exc} curves after annealing at 135 – 150 °C in Figure 2 are almost identical. During annealing at higher temperatures in the range of 155 °C – 180 °C, partial crystallization occurs as shown in the X-Ray Diffraction (XRD) patterns depicted in **Figure 3**, leading to a continuous decrease of the glass transition endotherm of $Ge_{15}Te_{85}$ at 140 °C, see

Figure 4a. Simultaneously, the C_p^{exc} value in the temperature range of 150 °C - 180 °C decreases while its slope increases showing signs of an emerging endotherm at higher temperatures that becomes most prominent at annealing temperatures of 180 °C – 190 °C. This emerging endotherm cannot be explained only by a decrease in $Ge_{15}Te_{85}$ content. Meanwhile, during annealing at 155 – 180 °C, the first crystallization peak decays until it eventually vanishes completely at 185 °C, while the second peak remains largely the same, see Figure 2b. At an annealing temperature of 190 °C the second peak also decreases until it vanishes at 200 °C, too. Interestingly, the more the first crystallization peak is reduced by annealing, the more prominent the second endotherm near 200 °C becomes.

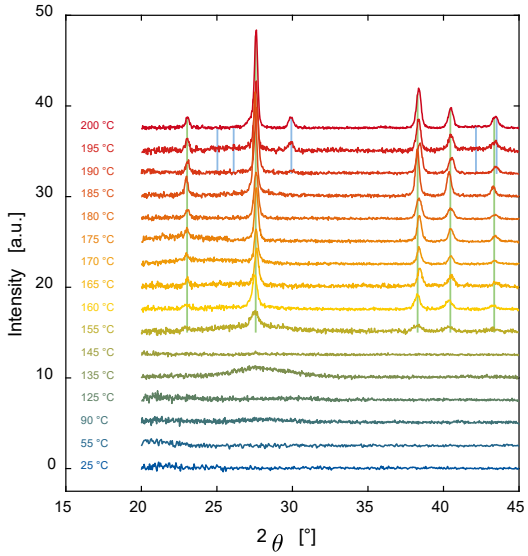

Figure 3: X-ray diffraction of $Ge_{15}Te_{85}$ powder after annealing at the indicated temperature for one hour. The powder for XRD and DSC measurements on $Ge_{15}Te_{85}$ was obtained from the same preparation process. The XRD scans show that crystallization firstly initiated during the one hour annealing at 155 °C. All peaks appearing up to an annealing temperature of 185 °C can be attributed to crystalline tellurium (light green vertical lines) [30]. These peaks become more pronounced for each annealing step up to 185 °C. The first GeTe diffraction peak that appears is the $(10\bar{2})$ peak at 29.9 ° [31] at an annealing temperature of 190 °C. It grows in intensity with increasing annealing temperature (see light blue vertical lines for GeTe reflections). A close-up around this peak can be found in the Supplementary Information (SI).

The multiple thermal events observed in Figure 2 a) and b) can be understood by considering that $Ge_{15}Te_{85}$ is a eutectic composition [32]. Once crystallized, it consists of 70 % crystalline tellurium and 30 % crystalline GeTe. Hence, the two crystallization events in Figure 2 could be related to the crystallization of these two crystalline phases. Support for this hypothesis is found in Ref. [33] and others, where tellurium was found to crystallize first. This is confirmed

by the X-ray diffraction (XRD) data presented in Figure 3. Here, as in the DSC-measurements from Figure 2, first signs for crystallization are found for an annealing temperature of 155 °C when the first diffraction peaks start to appear. This is also the annealing temperature where the glass transition endotherm of $Ge_{15}Te_{85}$ starts to decrease, see Figure 2 and 4a. All diffraction peaks are attributed to crystalline tellurium (space group: 152, [30]) up to an annealing of 185 °C, which confirms that tellurium crystallizes first. This is in line with changes in the excess heat capacity C_p^{exc} curves, where only the first crystallization peak is affected by annealing as an increasing fraction of tellurium is crystallized during annealing. Finally, at an annealing temperature of 190 °C or higher, diffraction peaks for GeTe (space group: 160, [31]) appear and increase up to an annealing temperature of 200 °C. For a close-up around the most prominent GeTe reflection, see Figure S1 in the Supplementary Information (SI). Simultaneously, the second crystallization peak in C_p^{exc} curves decreases and vanishes at 200 °C. For more details, see Figure S2 (SI). By combining the findings from XRD and DSC, the first crystallization peak can be attributed to the crystallization of tellurium, while the second crystallization peak is attributed to the crystallization of GeTe.

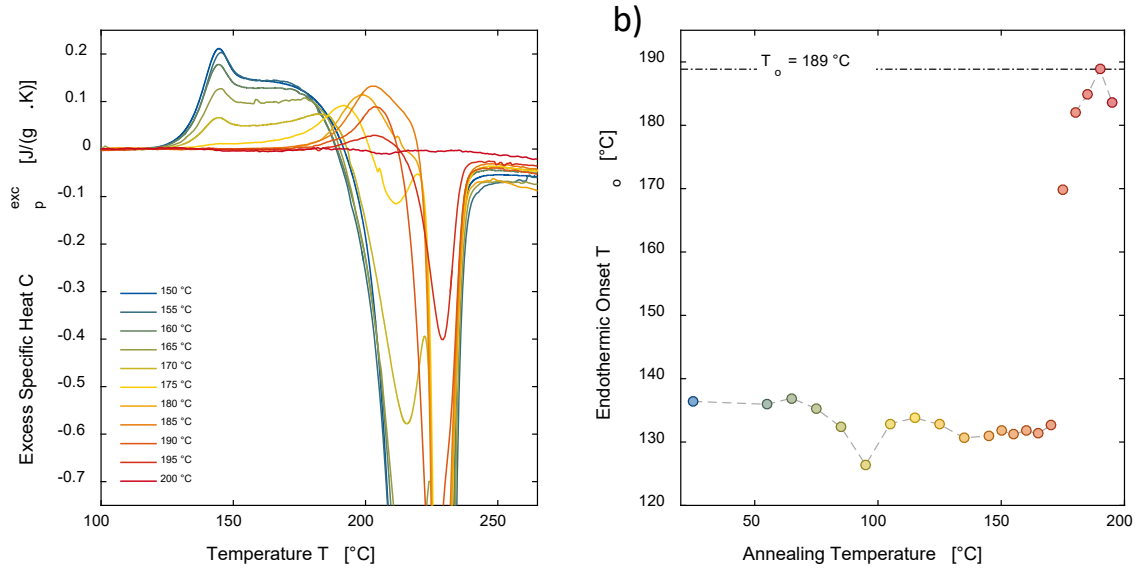

Figure 4: a) Close-up of excess heat capacity curves for the highest annealing temperatures from Figure 2. When the annealing temperature is increased from 155 °C to 185 °C, the first crystallization peak disappears and instead an endotherm develops. This first crystallization peak has been attributed to the formation of crystalline tellurium from XRD data, while the second peak is assigned to GeTe crystallization. The corresponding DSC peak is influenced notably only at an annealing of 190 °C or higher and the crystallization peak disappears at an annealing at 200 °C. After annealing at 200 °C for one hour, the sample has completed crystallization. b) Endothermic onset temperature after annealing at the indicated temperatures for one hour. At low annealing

temperatures, this onset is the glass transition of as-deposited $Ge_{15}Te_{85}$. It is decreasing up to an annealing of 95 °C when the shadow glass transition and glass transition merge and subsequently jumps up at 105 °C. The onset temperature experiences a rapid jump when the annealing temperature increases from 170 °C to 175 °C. When the tellurium has crystallized (at T_{an} = 185 °C, see Figure 3 and Figure 4a) the endotherm can only be caused by the glass transition of the remaining amorphous material which is approaching the composition of GeTe. Therefore, the measured onset temperature of 189 °C provides an estimate for the glass transition temperature T_g of GeTe.

2. Discussion

DSC and XRD data demonstrate that crystallization in $Ge_{15}Te_{85}$ takes place in two distinct processes where the crystallization of tellurium is followed by that of GeTe. By proper annealing, a volume fraction x of tellurium can be crystallized without crystallizing GeTe, see Figure 3. This volume fraction is thus removed from the remaining amorphous material leading to a composition change according to $Ge_{15}Te_{(85-x)}$ by the diffusion of germanium into the amorphous phase and tellurium into the crystal. This means that the composition of the amorphous material changes towards GeTe, as can be seen in **Figure 5**.

As soon as the composition starts changing, an unexpected endotherm near 200 °C develops which must be caused by the glass transition of the remaining (glassy) amorphous material that was formed upon cooling the UCL after annealing, whose presence is demonstrated in **Figure S3** (SI). Hence, from the onset temperature of this endotherm, the glass transition temperature T_g of the remaining amorphous material can be deduced, see Figure 4b. Upon the crystallization of tellurium, the high temperature endotherm and its onset shift to higher temperatures, as shown in Figure 4a and b, as the composition of the remaining amorphous phase $Ge_{15}Te_{(85-x)}$ shifts towards the composition of GeTe, see **Figure 6**. Therefore, the glass transition temperature of the PCM GeTe is then defined as the maximum onset of the high temperature endotherm at ~ 190 °C as depicted in Figure 4b. It is discussed in the SI, if the composition of $Ge_{50}Te_{50}$ can finally be reached and how robust the observed glass transition temperature is to a change in composition.

While the glass transition of pure GeTe is obscured by crystallization, see Figure 1, the glass transition of GeTe becomes observable in annealed $Ge_{15}Te_{85}$, see Figure 2 and 4a, as here the onset of crystallization of GeTe is postponed by ~ 40 °C while the crystallization peak temperature is postponed by 10 °C. There could be two reasons for this delay. On the one hand, as can be seen in Figure 6, the size of the GeTe containing areas is within the tens of nanometers range. This size might be small enough for confinement effects to become important. On the other hand, the crystallization of GeTe in annealed $Ge_{15}Te_{85}$ is made possible by the diffusion processes involved due to tellurium crystallization. Therefore, it may take some time until the Ge content becomes high enough for GeTe to initialize crystallization.

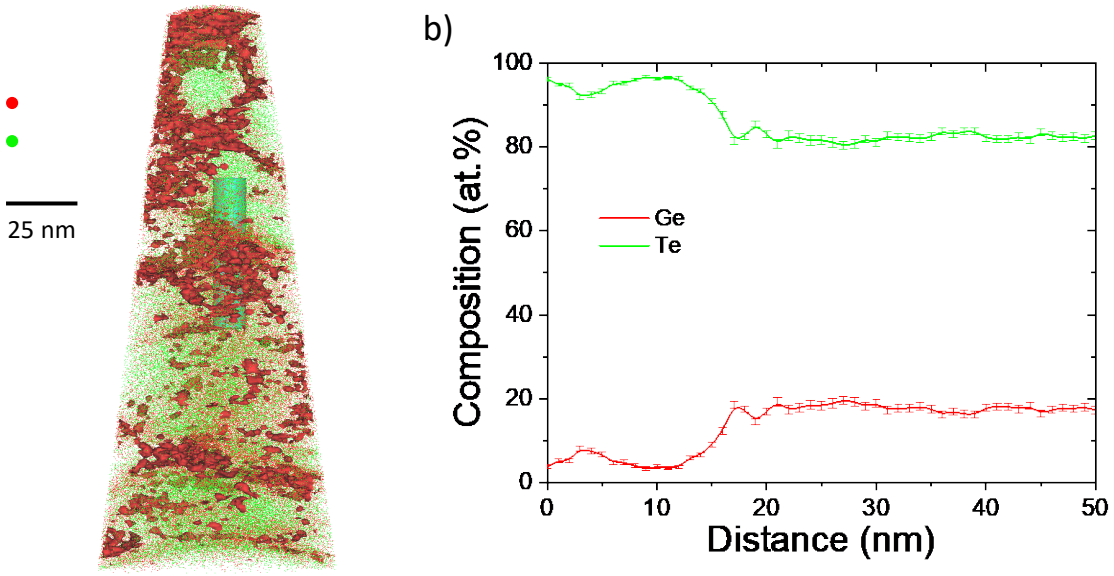

Figure 5: Atom Probe Tomography (APT) of locally detected ions of a $Ge_{15}Te_{85}$ sample annealed at 170 °C for 1 h. The powder for APT, XRD and DSC measurements of $Ge_{15}Te_{85}$ was obtained in the same preparation process. In a), tellurium is shown in green and germanium in red. Regions of crystallized tellurium are clearly visible. Regions containing more than 20 % of germanium are enclosed by a red iso-surface. The concentration profile within the turquoise cylinder is shown in b). The germanium content of the remaining amorphous phase outside the tellurium crystal shows a constant base level of about 20 % after a transition region of about 5 nm.

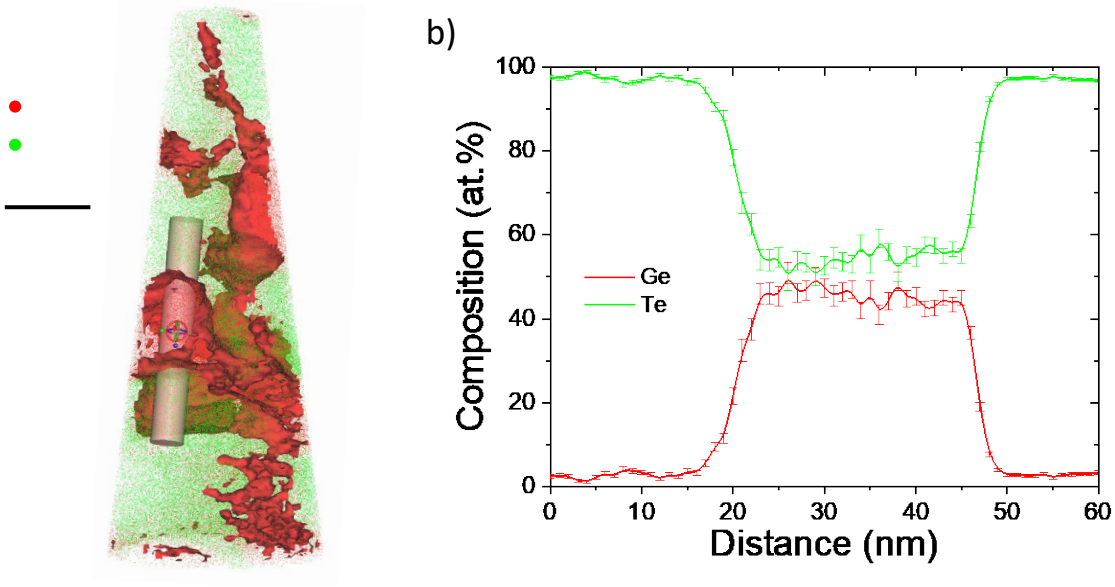

Figure 6: Atom Probe Tomography (APT) of locally detected ions of a $Ge_{15}Te_{85}$ sample annealed at 200 °C for 1 h. The powder for APT, XRD and DSC measurements of $Ge_{15}Te_{85}$ was obtained in the same preparation process. In a), the local distribution of tellurium (green) and germanium (red) is shown. Regions of crystallized tellurium and GeTe are clearly distinguishable. Regions containing more than 30 % of germanium are enclosed by a red iso-surface. The concentration profile within the cylinder in a) is shown in b). The germanium concentration outside the tellurium crystals has reached the final concentration of GeTe within experimental uncertainty (error bars in b) indicate the standard deviation of the various composition values determined in the selected area).

3. Conclusion

In this study, we have shown at first that a direct measurement of the calorimetric glass transition of pure GeTe fails because the glass transition is obscured by crystallization (Figure 1), just as it was found previously in another MVB showing material ($Ge_2Sb_2Te_5$) [22]. Therefore, we have explored an alternative route. We studied $Ge_{15}Te_{85}$, a eutectic composition that transforms during crystallization into tellurium and GeTe where the tellurium crystallizes first and GeTe crystallizes afterwards. Increasing the annealing temperature leads to tellurium crystallization, which in turn shifts the local and average composition of the remaining amorphous material from the initial $Ge_{15}Te_{85}$ towards that of GeTe (also see SI). As the remaining amorphous material approaches the composition of GeTe, a high temperature endotherm develops which is identified to be the glass transition of this material. This endotherm serves as the basis for approximating the glass transition temperature T_g for GeTe to be around 190 °C.

4. Experimental Section/Methods

Powders for DSC, XRD, TEM and APT measurements of $Ge_{15}Te_{85}$ and GeTe were prepared from stoichiometric targets by magnetron sputter deposition at a base pressure of 3×10^{-6} mbar. The composition was confirmed via Scanning Electron Microscopy (SEM) in a FEI Helios Dual Beam FIB. The excess heat capacity C_p^{exc} was obtained in a PerkinElmer Diamond DSC by subtracting the crystalline rescan from the initial scan. The melting onset of pure Indium was used to calibrate the temperature at a constant heating ϑ as already reported in the Supplementary Information of Ref. [22].

The X-Ray Diffraction (XRD) data was measured with a Bruker D8 Discover Diffractometer in a reflection setup. The powder was placed on a single crystal Silicon substrate and illuminated with parallel Cu $K_{\alpha1}$ radiation at a fixed glancing angle of 1 °. The 2θ scans were obtained with a 1D LynxEye Silicon strip detector. For better comparability, the diffuse scattering background of the XRD scans was removed in Figure 3.

The needle-shaped Atom Probe Tomography (APT) specimen were prepared by a cross-beam focused ion beam (FIB, Helios NanoLab 650, FEI) according to the standard "lift-out" method. Low voltage (2 kV) was applied to the final APT specimen to remove any Ga contaminations due to the preparation process. APT characterization was carried out using a local electrode APT (LEAP 4000X Si, CAMECA) with an ultraviolet laser ($\lambda = 355$ nm, repetition rate of 200 kHz). The laser pulse energy was 5 pJ, the base temperature of the specimen was 40 K, the average detection rate was 1 % and the flight path of ions was 160 mm. Data reconstruction and analyses were processed using IVAS 3.8.0.

Acknowledgements

The authors acknowledge funding from the Deutsche Forschungsgemeinschaft (DFG) via the collaborative research center Nanoswitches (SFB 917) and in part by the Federal Ministry of

Education and Research (BMBF, Germany) in the project NEUROTEC (16ES1133 K). PL acknowledges funding from NSF-DMR grant No. 1832817. SW acknowledges the support of the DFG grant No. 422219280. SS acknowledges funding from Fonds der Chemischen Industrie. Support with XRD measurements by Tobias Strop is gratefully appreciated as well as the supervision of the APT setup by Oana Cojocaru-Miredin and by Svitlana Taranenko. Jean-Marc Joubert is gratefully acknowledged for conducting and providing us with the CALPHAD calculations of the stable and metastable phase diagrams and all helpful discussions and comments. We thank the anonymous reviewers for critically reading the manuscript and suggesting improvements concerning the stoichiometry of the glassy phase, whose T_g we determine.

Received: ((will be filled in by the editorial staff))
Revised: ((will be filled in by the editorial staff))
Published online: ((will be filled in by the editorial staff))

References

[1] M. Wuttig, N. Yamada, Nat. Mater., 6 (2007) 824-832.
[2] D. Lencer, M. Salinga, B. Grabowski, T. Hickel, J. Neugebauer, M. Wuttig, Nat. Mater., 7 (2008) 972.
[3] M. Zhu, O. Cojocaru-Mirédin, A.M. Mio, J. Keutgen, M. Küpers, Y. Yu, J.-Y. Cho, R. Dronskowski, M. Wuttig, Adv. Mater., 30 (2018) 1706735.
[4] J.Y. Raty, M. Schumacher, P. Golub, V.L. Deringer, C. Gatti, M. Wuttig, Advanced Materials, 31 (2019) 1806280.
[5] M. Wuttig, V.L. Deringer, X. Gonze, C. Bichara, J.Y. Raty, Adv. Mater., 30 (2018) 1803777.
[6] B.J. Kooi, M. Wuttig, Adv. Mater., 32 (2020) 1908302.
[7] J. Pries, O. Cojocaru-Miredin, M. Wuttig, MRS Bull., 44 (2019) 699-704.
[8] A. Sebastian, M. Le Gallo, D. Krebs, Nat. Commun., 5 (2014) 4314.
[9] M. Salinga, E. Carria, A. Kaldenbach, M. Bornhöfft, J. Benke, J. Mayer, M. Wuttig, Nat. Commun., 4 (2013) 2371.
[10] D. Turnbull, Contemp. Phys., 10 (1969) 473-488.
[11] S. Wei, Z. Evenson, M. Stolpe, P. Lucas, C.A. Angell, Sci. Adv., 4 (2018) eaat8632.
[12] S. Wei, C. Persch, M. Stolpe, Z. Evenson, G. Coleman, P. Lucas, M. Wuttig, Acta Mater., 195 (2020) 491-500.
[13] J.C. Mauro, Y. Yue, A.J. Ellison, P.K. Gupta, D.C. Allan, PNAS, 106 (2009) 19780-19784.
[14] C.A. Angell, Science, 267 (1995) 1924-1935.
[15] S. Wei, P. Lucas, C.A. Angell, MRS Bull., 44 (2019) 691-698.
[16] M. Chen, K.A. Rubin, Proc. SPIE, 1078 (1989).
[17] Y.M. Chen, G.X. Wang, L.J. Song, X. Shen, J.Q. Wang, J.T. Huo, R.P. Wang, T.F. Xu, S.X. Dai, Q.H. Nie, Cryst. Growth Des., 17 (2017) 3687-3693.
[18] B. Chen, D. de Wal, G.H. ten Brink, G. Palasantzas, B.J. Kooi, Cryst. Growth Des., 18 (2018) 1041-1046.
[19] M.H.R. Lankhorst, J. Non-Cryst. Solids, 297 (2002) 210-219.
[20] M.K. Santala, B.W. Reed, S. Raoux, T. Topuria, T. LaGrange, G.H. Campbell, Appl. Phys. Lett., 102 (2013) 174105.
[21] Y. Chen, S. Mu, G. Wang, X. Shen, J. Wang, S. Dai, T. Xu, Q. Nie, R. Wang, Appl. Phys. Express, 10 (2017) 105601.
[22] J. Pries, S. Wei, M. Wuttig, P. Lucas, Adv. Mater., 31 (2019) 1900784.
[23] J.A. Kalb, M. Wuttig, F. Spaepen, J. Mater. Res., 22 (2007) 748-754.

[24] J. Pries, S. Wei, F. Hoff, P. Lucas, M. Wuttig, Scr. Mater., 178 (2020) 223-226.
[25] Y.Z. Yue, S.L. Jensen, J. deC. Christiansen, Appl. Phys. Let., 81 (2002) 2983-2985.
[26] C.A. Angell, Y. Yuanzheng, W. Li-Min, R.D.C. John, B. Steve, M. Stefano, J. Phys. Condens. Matter, 15 (2003) S1051.
[27] L. Hu, Y. Yue, The Journal of Physical Chemistry C, 113 (2009) 15001-15006.
[28] G.W. Scherer, Relaxation in Glass and Composites, Wiley, New York, 1986.
[29] S. Wei, P. Lucas, C.A. Angell, J. Appl. Phys., 118 (2015) 034903.
[30] C. Adenis, V. Langer, O. Lindqvist, Acta Crystallogr. C Cryst. Struct. Commun., 45 (1989) 941-942.
[31] P. Bauer Pereira, I. Sergueev, S. Gorsse, J. Dadda, E. Müller, R.P. Hermann, Phys. Status Solidi B, 250 (2013) 1300-1307.
[32] A. Schlieper, Y. Feutelais, S.G. Fries, B. Legendre, R. Blachnik, Calphad, 23 (1999) 1-18.
[33] R. Sengottaiyan, N. Saxena, K.D. Shukla, A. Manivannan, J. Phys. D Appl. Phys., 53 (2020) 025108.

J. Pries, Y. Yu, P. Kerres, M. Häser, S. Steinberg, F. Gladisch, S. Wei, P. Lucas, M. Wuttig*

Approaching the Glass Transition Temperature of GeTe by Crystallizing $Ge_{15}Te_{85}$

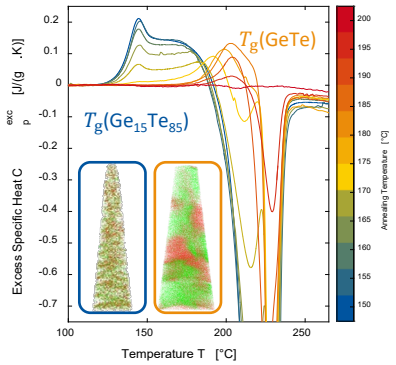

When the eutectic composition $Ge_{15}Te_{85}$ crystallizes, it transforms into tellurium and GeTe during two distinct crystallization events. As tellurium crystallizes first, the composition of the remaining amorphous material changes towards that of GeTe. During that shift in composition, an endotherm of a glass transition develops whose onset approaches the glass transition temperature T_g of GeTe.

Supporting Information

Approaching the Glass Transition Temperature of GeTe by Crystallizing $Ge_{15}Te_{85}$

*Julian Pries, Yuan Yu, Peter Kerres, Maria Häser, Simon Steinberg, Fabian Gladisch, Shuai Wei, Pierre Lucas, Matthias Wuttig**

1. Details on X-Ray Diffraction

In Figure S1 precision XRD (PXRD) patterns of $Ge_{15}Te_{85}$ annealed at the indicated temperatures for one hour are presented. The data presented in Figure S1 and S2 was obtained at room temperature by a Stoe StadiP powder diffractometer utilitzing Cu_{α} radiation. The graph gives a close-up around the most prominent GeTe peak at 29.9 ° in order to determine at what annealing temperature the first crystalline GeTe occurs. After annealing at 175 – 185 °C for one hour, no sign of GeTe crystallization is found. When the annealing temperature becomes 190 °C, the region at 29.9 ° shows slightly increased relative intensity, indicating that only little GeTe has crystallized. Annealing at 195 °C or 200 °C yields a clear increase in relative intensity, indicating that a much larger amount of GeTe has crystallized.

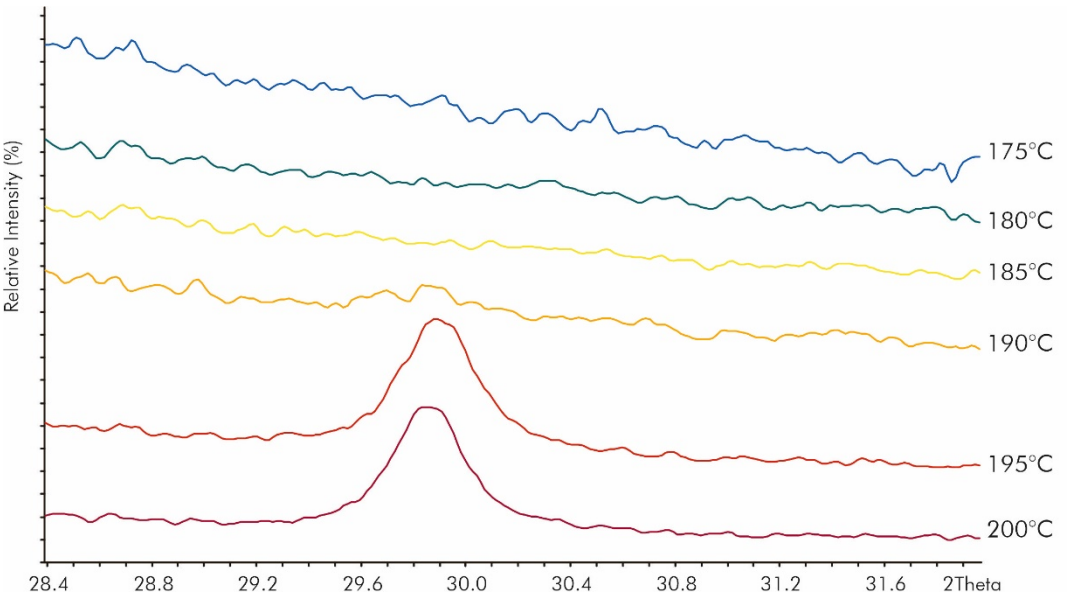

Figure S1: Annealed $Ge_{15}Te_{85}$ precision XRD pattern close-up of the region of the most pronounced peak of GeTe, see Figure 3 (main text). The $Ge_{15}Te_{85}$ samples were annealed at the indicated temperatures for one hour each.

In Figure S2, a precision X-ray diffraction (PXRD) pattern for $Ge_{15}Te_{85}$ annealed at 200 °C for one hour is shown. This pattern is used for a Rietveld refinement for the theoretical patterns of GeTe [1] and Te [2]. From this refinement a phase fraction of 85 % crystalline tellurium and 15 % GeTe was obtained that corresponds to a over all composition of $Ge_{12.75}Te_{85}$, if about 5 % of the sample were still amorphous. The PXRD and the Rietveld refinement however are not sensitive for amorphous material. PXRD therefore suggests that a small amount of amorphous phase remains after the annealing at 200 °C for one hour.

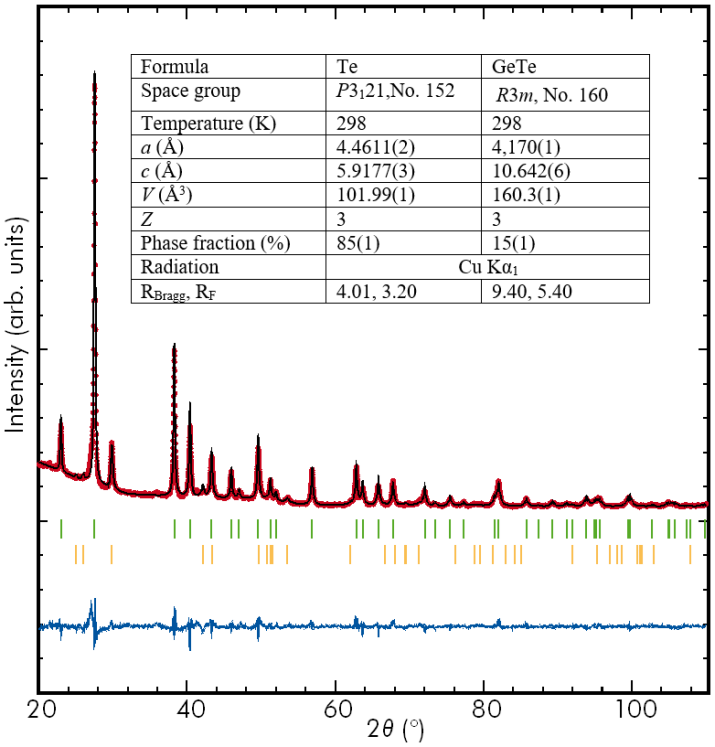

Figure S2: Rietveld refinement of the PXRD pattern of $Ge_{15}Te_{85}$ annealed at 200 °C for one hour. The Rietveld refinement was started based on the theoretical patterns of GeTe [1] and Te [2], and was accomplished employing the FullProf_Suite [3].

2. Microscopic Insights

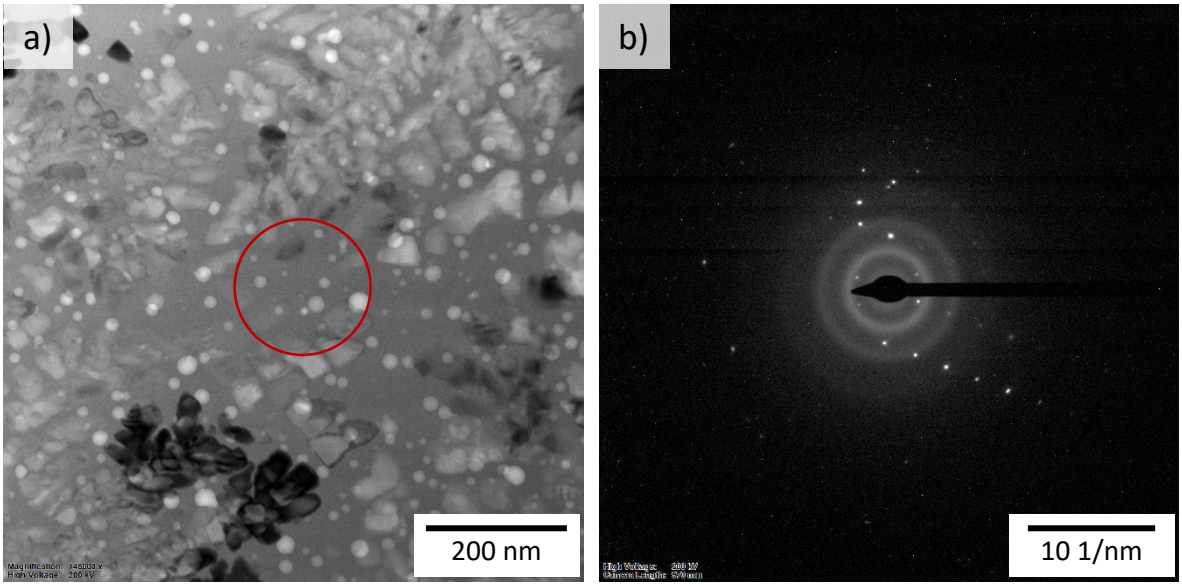

Figure S3: Transmission electron microscopy (TEM) image a) and selective area electron diffraction (SAED) image b) of $Ge_{15}Te_{85}$ annealed at 185 °C for 1 h. The TEM lamella was prepared in a FEI Helios Dual Beam FIB and measured at a FEI Tecnai F20 TEM. The bright and dark areas of dendritic shape in a) are identified as crystallized tellurium. The red circle in a) indicates the selected area for electron diffraction (SAED). The resulting SAED pattern is shown in b). Only reflections of crystalline tellurium are found, no reflections of GeTe are present. The diffuse rings around the beam center are caused by scattering of the electron beam on amorphous material, which demonstrates the presence of the amorphous phase in the sample.

3. Composition of the Remaining Amorphous Phase

When the eutectic composition of $Ge_{15}Te_{85}$ is cooled from the liquid below the eutectic temperature and only tellurium crystallizes, the composition of the remaining amorphous/liquid phase at a given temperature should change according to the extrapolated liquidus line (Figure S4, dashed light blue line, linearly extrapolated as a rough estimate) of the tellurium rich liquid. In this case, a remaining amorphous/liquid phase composition could only reach that of $Ge_{50}Te_{50}$ at the temperature where this extrapolation reached a tellurium content of 50 %. This would be the case at a temperature of roughly 110 °C. This means that for all the annealing temperatures applied in the main text where signs of tellurium crystallization are observed (155 – 200 °C), the remaining composition would not reach the $Ge_{50}Te_{50}$ composition but instead show higher concentrations in tellurium. Thus, the T_g value that is specified in the main text could potentially deviate significantly from the T_g value of pure GeTe ($Ge_{50}Te_{50}$). The question now it by how much the glass transition temperatures varies with a variation in composition of the remaining amorphous phase. To find an answer to this question, we can make use of the fact, that the lower the annealing temperature, the higher the germanium content of the remaining amorphous phase that can be reached and thus the closer it is to GeTe.

Therefore, additional crystallization experiments at an annealing temperature as low as possible, i.e. 155 °C was conducted, see Figure S5 and the resulting endothermic onset temperature is measured. The annealing temperature of 155 °C was chosen because it is the lowest annealing temperature at which crystallization of tellurium was observed within one hour (main text). From the difference in onset temperature between the annealing at 155 °C and 185 °C, the deviation of the approximated value for the glass transition temperature T_g (main text) to the T_g in pure GeTe can be estimated. Following the extrapolation from Figure S4, at an annealing temperature of 185 °C, the final germanium content in the remaining amorphous phase would be approximately 40 %, while at 155 °C the final germanium content could be approximated to be about 44 %. Note, that the prediction of the final composition is strongly dependent on the exact shape of the extrapolation, which will be addressed below.

The goal for the new annealing experiment at 155 °C is to heat-treat the as-deposited $Ge_{15}Te_{85}$ as long as needed to crystallize as much tellurium as possible. The onset temperature of the glass transition can be measured from the maximum endotherm that has formed. The resulting excess heat capacity C_p^{exc} curves are presented in Figure S5. Here, the highest endotherm occurs after an annealing for 3600 min at 155 °C, while after 7000 min the sample has completely crystallized. After an annealing of 3600 min, the onset temperature of the high temperature endotherm is 191 °C. This value is almost identical to the value found in the main text of 189 °C for an annealing at 185 °C. Therefore, it can be concluded that the glass transition temperature T_g approximated in the main text is still a good estimate for the T_g of GeTe. This also means, that apparently, the glass transition temperature is rather robust with respect to moderate composition changes in the vicinity of GeTe.

We note in passing that the shapes of the endotherm at the annealing temperature at 155 °C and 185 °C (main text) differ. The reason that the endotherm in Figure S5 develops a much higher endothermic overshoot as in the main text stems from the annealing termpature here being much lower than the standard glass transition temperature. This causes enthalpy relaxation (release) which in turn is compensated for during the reheating by a higher endotherm [5]. Therefore, this difference in the shape of the endotherm once more supports

the finding that this endotherm is indeed the glass transition of the remaining amorphous phase.

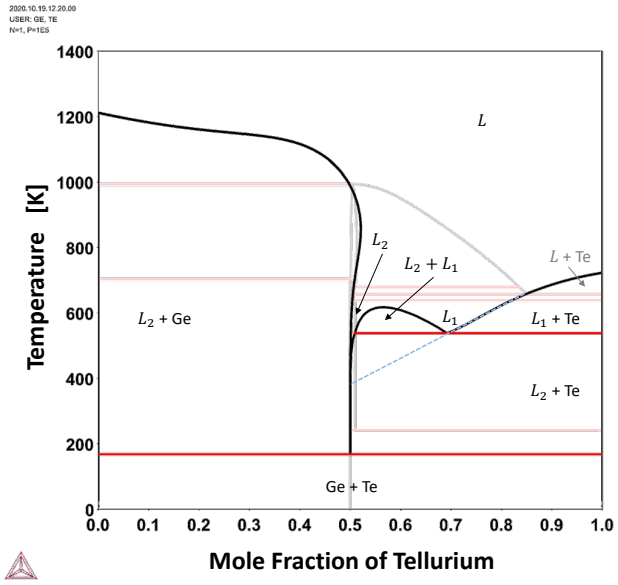

Figure S4: CALPHAD calculation of the phase diagram of germanium and tellurium based on Ref. [4]. Grey and light red lines indicate the phase boundary lines of the stable phase diagram which is in accordance of Ref. [4]. Based on these data, a second phase diagram is calculated for all phases except for the crystalline/stable phases of GeTe leading to the black and red lines. Note, some of the stable boundary lines (grey) are covered by metastable lines (black). This metastable phase diagram reveals a monotectic line (red) at 538 K (265 °C). When the liquid L_1 is cooled below the monotectic line, a monotectic reaction of L_1 → L_2 + Te takes place, where L_i denotes different liquid phases of different composition and Te is crystalline tellurium. Below the monotectic line, the liquid L_2 features a composition of almost $Ge_{50}Te_{50}$. The extrapolation of the tellurium rich liquidus line (light blue dashed line) from the eutectic point is only a guide to the eye.

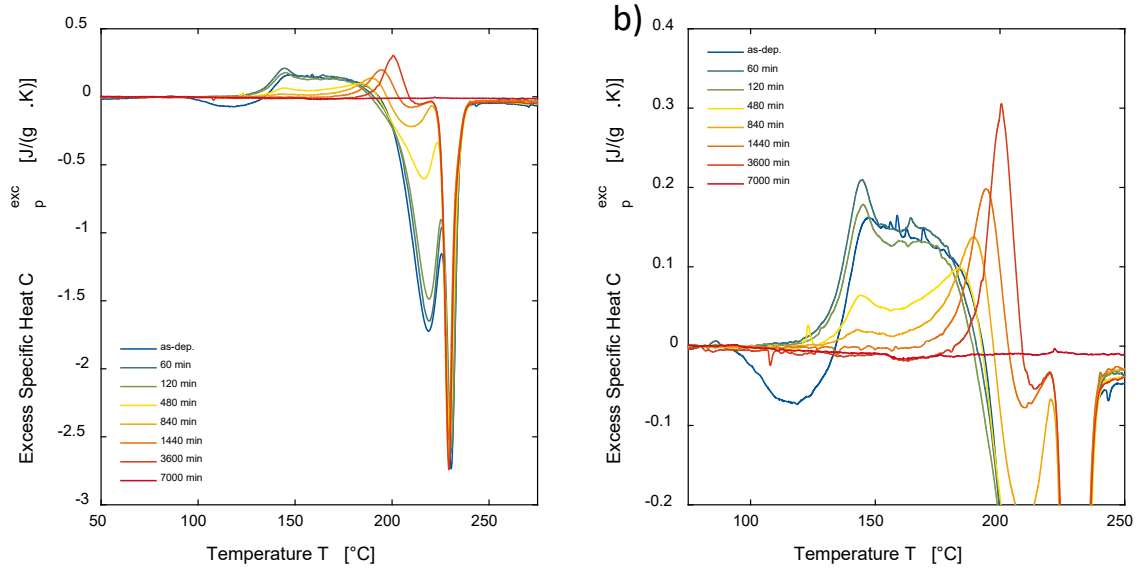

Figure S5: Excess heat capacity C_p^{exc} of amorphous $Ge_{15}Te_{85}$ powder obtained by DSC after an annealing at 155 °C for the indicated duration followed by heating with a rate ϑ_h of 40 K/min. Crystallization consists of two individual processes, which are assigned to tellurium- and GeTe-crystallization, respectively. As the tellurium is

crystallized during annealing, the glass transition endotherm of $Ge_{15}Te_{85}$ ceases and a new endotherm at around 200 °C forms. The onset temperature after an annealing of 3600 min at 155 °C is 191 °C, which is very close to the approximated value for the glass transition temperature of GeTe from in the manuscript. After annealing for 7000 min, the material has fully crystallized. b) is a close-up of a).

Until now a clarification on the exact composition of the amorphous phase whose T_g was determined in the main text is still missing as the prediction of the composition of the remaining amorphous phase after tellurium crystallization is dependent on the exact shape of the extrapolated liquidus line. A CALPHAD-based extrapolation of the tellurium-rich liquidus line should yield satisfactory accuracy. We are not aware of any CALPHAD calculations on the phase diagram of germanium and tellurium other than Ref. [4]. These calculations do not contain a liquidus line extrapolation of the tellurium rich liquid. Therefore new CALPHAD calculations were executed for the stable and metastable phase diagram of germanium and tellurium. An overlay of both phase diagrams is presented in the aforementioned Figure S4. The stable phase diagram is in good agreement with Ref. [4].

The metastable phase diagram is based on the same data as in Ref. [4], however all stable (crystalline) phases of GeTe were excluded from the calculations. With this metastable phase boundary lines, the liquidus line of the tellurium rich liquid phase is extrapolatable down to 265 °C, which is about 120 °C below the eutectic temperature. At 265 °C, a monotectic line is reached and a miscibility gap of two liquids of different composition is observed, see Figure S4. This miscibility gap in the liquid phase is caused by the high stability of the liquid at the composition of $Ge_{50}Te_{50}$. This is testified by the measured enthalpy of mixing in the liquid phase at high temperatures [4], which justifies the use of an associate model with associate composition $Ge_{50}Te_{50}$ in the modelling of the liquid to describe the short-range order. The resulting calculated metastable miscibility gap depends apparently on details of the model, but the model itself is justified by the experimental data. Therefore, the presence of this metastable miscibility gap is trustworthy. In any case, the high stability of the liquid at GeTe composition proved experimentally leads to a rapid convergence of the liquid composition towards $Ge_{50}Te_{50}$.

This indicates that a liquid phase of the over all composition of $Ge_{15}Te_{85}$ should transform into the liquid phase L_2 and crystalline tellurium when the temperature is lowered below 265 °C, see Figure S4. According to the phase diagram in Figure S4, the composition of the liquid phase L_2 at the annealing temperatures from the main text (up to 200 °C) is almost exactly $Ge_{50}Te_{50}$. When tellurium crystallizes at these temperatures, the remaining amorphous phase is in or close to the undercooled liquid state (UCL) where atomic mobility is high. Therefore, it is most likely that the initial as-deposited amorphous phase transforms into the liquid phase L_2 of composition $Ge_{50}Te_{50}$ while tellurium is crystallizing upon annealing.

If indeed the amorphous phase of $Ge_{15}Te_{85}$ undergoes a phase transition directly into crystalline tellurium and the liquid L_2, the remaining amorphous phase should approach the composition of $Ge_{50}Te_{50}$ for all annealing temperatures applied in the main text (at sufficient annealing time). This could explain why the glass transition temperature measured does not depend on the anneling temperature except for the difference in the shape of the endotherms, as discussed above.

References

[1] J. Goldak, C.S. Barrett, D. Innes, W. Youdelis, The Journal of Chemical Physics, 44 (1966) 3323-3325.
[2] P. Cherin, P. Unger, Acta Crystallographica, 23 (1967) 670-671.
[3] J. Rodríguez-Carvajal, Physica B: Condensed Matter, 192 (1993) 55-69.
[4] A. Schlieper, Y. Feutelais, S.G. Fries, B. Legendre, R. Blachnik, Calphad, 23 (1999) 1-18.
[5] G.W. Scherer, Relaxation in Glass and Composites, Wiley, New York, 1986.